

# Large-scale multilayer architecture of single-atom arrays with individual addressability

Malte Schlosser, Sascha Tichelmann, Moritz Hambach,  
Daniel Ohl de Mello, Dominik Schöffner, and Gerhard Birkl\*  
*Institut für Angewandte Physik, Technische Universität Darmstadt,  
Schlossgartenstraße 7, 64289 Darmstadt, Germany*

(Dated: December 15, 2024)

## Abstract

We report on the realization of a novel platform for the creation of large-scale 3D multilayer configurations of planar arrays of individual neutral atoms: a microlens-generated Talbot optical lattice. We demonstrate the trapping and imaging of rubidium atoms in multiple Talbot planes and prepare a single atom in 161 sites of a selected plane. We present interleaved single-atom arrays with dynamic position control and single-site resolved addressing of spin states. The single beam illumination of a microlens array constitutes a structurally robust and wavelength-universal method for the realization of 3D atomic arrays with favourable scaling properties due to the inherent self-imaging of the focal array through the Talbot effect. Geometry, trap size, and unit cell dimensions are configurable in the micrometer regime with immediate applications in quantum science and technology.

## INTRODUCTION

Outstanding progress in atomic physics has paved the way for experiments which probe and exploit the laws of quantum mechanics at the single quantum level [1, 2]. A cornerstone are neutral atoms trapped by light [3], which constitute a versatile experimental platform where internal and external degrees of freedom can be coherently manipulated and interactions are tunable by all optical means. This comprehensive control is the key element of forefront research in an extensive field including quantum chemistry [4, 5], quantum metrology [6], interferometry [7] and sensing [8, 9], quantum information processing [10–12] and quantum simulation [13–18].

A natural focus are multi-site geometries created by optical lattices [15–17, 19, 20] and arrays of optical tweezers [21–29]. The former serve as carrier for a myriad of isolated probes, thereby taintlessly boosting signal and sensitivity, as well as they provide pure many-body systems with controllable tunnelling. An indispensable tool are quantum gas microscopes which give access to local observables with single site resolution. Fostered by the ability to filter the atom number per site in a Mott insulator for bosons and a Fermi degenerate gas for fermions, optical lattices enable the top-down implementation of condensed matter models with several hundred atoms [15, 16] and the realization of record optical clocks [30]. Flexible arrays of optical tweezers created by focused laser beams decouple trap size and separation as well as array geometry from the constraint of interference, which is imposed on optical lattices. Their inherently resolved trapping sites are adaptable to either hold a bulk of atoms [31, 32], number resolved ensembles [33, 34], or single atoms [35, 36] and can be composed from multiple colours of laserlight [5, 22, 37]. Straightforward dynamic position control represents a fruitful tool which facilitates the coherent transport of quantum states [38, 39] and the seminal assembly of defect free sub-arrays [40–43]. Thus, arrays of individually controlled microtraps lend themselves to the bottom-up engineering of quantum systems with configurable on-demand interactions from tunnel-coupled [44–47] to Rydberg physics [10, 12, 13, 48]. Pioneering implementations realized the fundamental building blocks of the Bose-Hubbard [44] and the Hubbard model [45], the formation of a molecule [5] and small spin systems with Rydberg interactions ranging from dynamically coupled to blockaded [24, 25, 48].

Compared to optical lattices, atom numbers have been limited and remained below one hun-

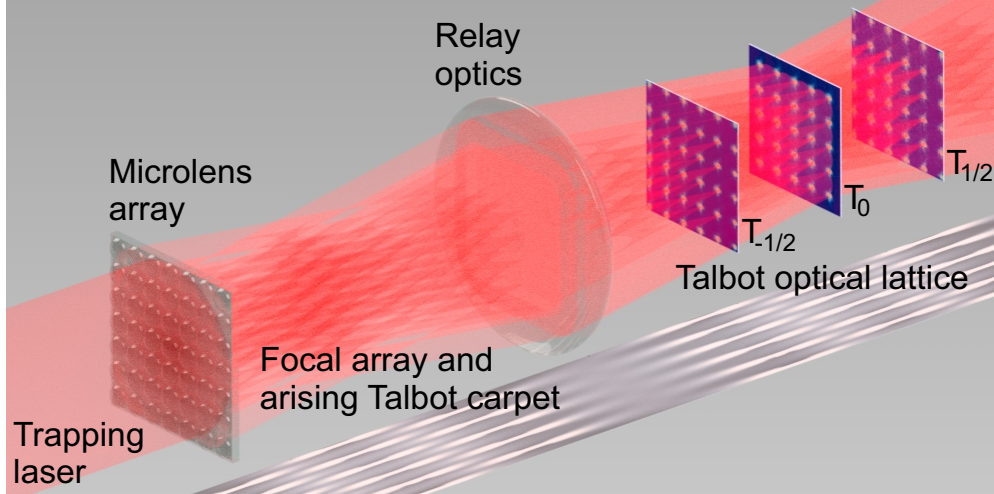


FIG. 1. Illustration of the microlens-array generated Talbot optical lattice. The periodic spot pattern of the focal plane gives rise to the formation of a 3D Talbot carpet. After reimaging and demagnification, we obtain a site-resolved multilayer lattice of 2D periodic microtrap arrays formed from regular self-images of the generating focal plane. The resulting geometry is visualised with averaged fluorescence images of  $^{85}\text{Rb}$  atoms stored in the reimaged focal plane  $T_0$  and the planes  $T_{\pm 1/2}$  (see text for details).

dred. For future progress, scalability is pivotal. In this article, we address this evident need for a configurable large scale implementation with a novel platform. We create quantum registers of individual atoms using the microtraps generated by the focal spots of a microlens array (MLA) and harness the Talbot effect [49] to multiply this 2D periodic configuration to a multilayer architecture in the third dimension. This Talbot optical lattice [50, 51] exhibits excellent scalability as it is built in parallel from a microfabricated source element with thousands of lenslets and the self imaging effect which comes at no additional cost.

## MICROLENS GENERATED TALBOT OPTICAL LATTICE

Figure 1 visualizes the experimental platform: The source element is a quadratic grid MLA of  $166 \times 166$  refractive lenslets with a pitch of  $30.0(3) \mu\text{m}$ , a diameter of  $26.5(20) \mu\text{m}$ , and a radius of curvature of  $42(2) \mu\text{m}$ . A subset of lenslets is illuminated by the trapping laser, which emits light at wavelength of  $798.6 \text{ nm}$  and has a beam waist of  $200(2) \mu\text{m}$  at the position of the MLA. The periodic spot pattern in the focal plane is the origin of

a 3D Talbot carpet, which exhibits self-images of the generating array – Talbot planes – in the axial dimension [49, 52, 53]. The separation of regular self-images is given by the Talbot length  $z_T = 2a^2/\lambda$ , which is a function of the spatial period  $a$ . Fractional self-images are found at fractional multiples of  $z_T$  and individual planes  $T$  are labeled according to their axial position normalized to  $z_T$  with  $T_0$  being the generating array. The focal array is reimaged and demagnified by the use of relay optics, which renders the pitch and the associated Talbot length configurable. A noticeable modification due to reimaging is the appearance of negative indexed Talbot planes which complete the symmetric 3D structure of the resulting Talbot optical lattice.

In this realization, we have used a generating trap array with trap pitch of  $a = 14.1(4) \mu\text{m}$  and trap waist of  $w_0 = 1.5(1) \mu\text{m}$ . Typical trap depths are on the order of  $k_B \cdot 1 \text{ mK}$ . The Talbot distance evaluates to  $z_T = 497(28) \mu\text{m}$ . This corresponds to an axial separation of  $z_T/2 = 248(14) \mu\text{m}$  of similar trap arrays since the planes  $T_0, T_{\pm 1/2}, T_{\pm 1} \dots$  reproduce the same in-plane geometry. We superimpose a standard magneto-optical trap and load the lattice sites with laser-cooled  $^{85}\text{Rb}$  atoms during a sequence of optical molasses. For the preparation of an atomic 2D Talbot register, the imaging system is focused to the selected plane and the atoms in all other planes are removed with a blow-away laser resonant to the cycling transition. Figure 1 exemplarily shows the averaged fluorescence of single atoms stored in the focal plane  $T_0$  and in the Talbot planes  $T_{\pm 1/2}$ . The trap-positions are stable and optically resolved which reveals the underlying periodic geometry.

## SINGLE ATOM QUANTUM REGISTER

Each 2D layer can serve as single atom quantum register with a readily scalable number of sites. For the experimental implementation presented in Figure 2, we have used a modified setup of 446 optical microtraps. We utilized a larger trapping laser beam of  $1923(21) \mu\text{m}$  with a wavelength set to  $796.3 \text{ nm}$  and a quadratic grid MLA of  $110.0(3) \mu\text{m}$  pitch. The lenslets are of  $106(2) \mu\text{m}$  diameter with a radius of curvature of  $0.86(4) \text{ mm}$ . This results in microtraps with a waist of  $1.5(1) \mu\text{m}$  and a configured pitch of  $10.3(3) \mu\text{m}$  in the utilized plane  $T_{-1/2}$ . Figure 2 gives (a) an averaged fluorescence image of a  $18 \times 18$  site detail and (b) a single shot revealing the fluorescence of individual atoms distributed over the trap array.

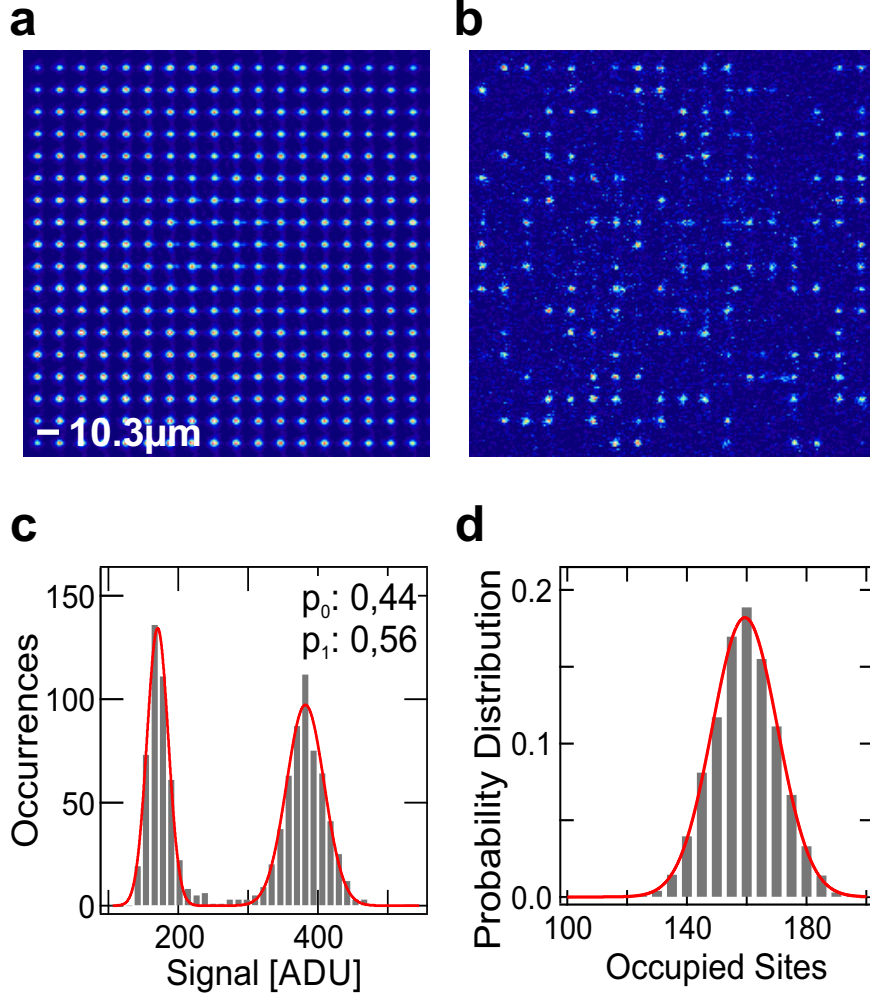


FIG. 2. Micro-optical realization of a  $10.3\ \mu\text{m}$  pitch quantum register with 446 sites. (a)  $18 \times 18$  site detail showing the averaged fluorescence at the resolved trapping positions. (b) In-situ detection of single  $^{85}\text{Rb}$  atoms at individual sites. (c) Histogram of the detected fluorescence data of a single trap. The peaks correspond to background and the fluorescence of a single atom, respectively. Two-atom events are blocked due to light assisted collisions. (d) Histogram of the total atom number per realization and binomial fit showing on average 161 traps loaded with one single atom each.

The preparation process based on light assisted collisions results in a heavily sub-Poissonian distribution stemming from the effect of collisional blockade [35]. Figure 2(c) exemplarily shows a histogram of the fluorescence recorded for a single site in consecutive experimental runs, which exhibits two distinct peaks corresponding to background light and the fluorescence of a single atom. A Gaussian fit to the data yields the probabilities for no-atom ( $p_0$ )

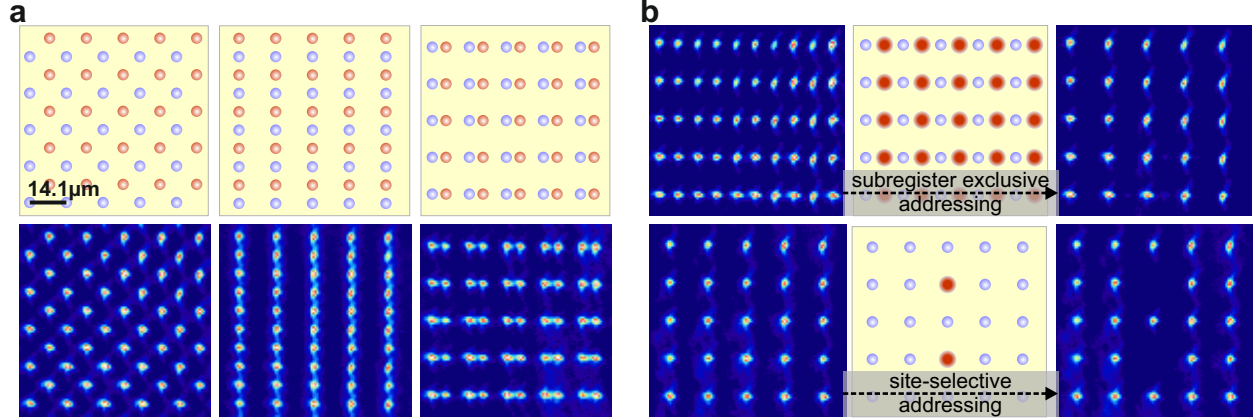


FIG. 3. All shown experiments have been performed utilizing the  $T_{1/2}$  Talbot plane. (a) Quantum registers with tunable atomic separation created from two interleaved Talbot lattices. The configuration is visualized by depicting the traps of the respective lattices in red and blue (top) and with averaged fluorescence images of stored atoms (bottom). The separation of neighbouring traps is from left to right:  $9.9(3) \mu\text{m}$ ,  $7.0(2) \mu\text{m}$ , and  $5.0(2) \mu\text{m}$ . (b) Addressing of stored atoms (illustration and averaged fluorescence images): (top) Subregister exclusive addressing is used to convert a spin polarized register ( $F = 2$ ) to a configuration of column-wise alternating spin states ( $F = 2$  and  $F = 3$ ). State selective detection records fluorescence for atoms in  $F = 2$  only. (bottom) Addressing of selected sites is used to remove selected atoms and create defects.

and one-atom ( $p_1$ ) events as given in the graph. In total, 390 sites feature a success rate for single atom preparation which is above the limit of 0.37 obtained from Poissonian statistics and on average 161 sites are loaded with an individual atom (Fig. 2(d)). We do not observe any two-atom events. Values of  $p_1 > 0.5$  indicate the presence of two-body collisional events which cause only one of the participants (instead of both) to leave the trap. This channel allows for the near-deterministic preparation of single atoms [23, 36]. We infer from maximum values of  $p_1 \approx 0.6$  that our current parameters correspond to a mixed regime with about 35 % of one-body losses.

## INTERLEAVED TALBOT LATTICES

The single atom quantum register of a selected plane can be extended to parallelized and interleaved geometries of multiple focused beam arrays by employing multiple MLAs as well

as by the irradiation of individual MLA with multiple trapping laser beams. This allows one to dynamically compose quantum registers with flexible site separation from superimposed moveable trap arrays [39].

Figure 3 shows configurations created from two interleaved sub-registers of the Talbot plane  $T_{1/2}$  with fundamental pitch of  $14.1(4) \mu\text{m}$ . These are implemented by expanding the setup used in the first section with a second trapping laser beam which irradiates the MLA under a modified incident angle, having a waist of  $202(2) \mu\text{m}$  and a frequency difference of  $30.0 \text{ MHz}$ . A relative difference  $0.36^\circ$  introduces an offset of half the trap pitch for the respective trap arrays.

Figure 3(a, left) shows a uniform arrangement that reduces the pitch by a factor of  $\sqrt{2}$  and forms a super-register with  $9.9(3) \mu\text{m}$  trap separation. Each site of a respective sub-register being equidistant to four sites of the other one. This symmetry may be broken by placing the traps in columns which creates a multitude of atom-chains with  $7.0(2) \mu\text{m}$  distance for the atoms within each column (Fig. 3(a, middle)). Furthermore, the trap positions can be tuned to favour pairs of atoms as demonstrated with a separation of  $5.0(2) \mu\text{m}$  for neighbouring atoms in Figure 3(a, right). In the current implementation, traps stay independent for a minimum separation of  $3 \mu\text{m}$  which is consistent with the trap waist.

Each of the sub-registers remains independently addressable by illuminating the respective microlenses, which in turn focus the light onto the trapping sites and thereby amplify the atom-light coupling. Moreover, if the addressing beam is set to spatial overlap with the trapping light it is auto-aligned with the traps while the spacing of interleaved quantum registers can be arbitrarily set within the limits given by trap pitch and trap waist.

In the experiments of Figure 3(b, top) we have used this technique for the spin-selective addressing of single atoms stored in sub-registers with a  $7.0(2) \mu\text{m}$  spacing. First, all atoms in the complete set of traps are initialized to  $F = 2$  state of the  $^{85}\text{Rb}$  ground state hyperfine manifold and state-selectively detected afterwards by removing the population of the  $F = 3$  hyperfine state prior to detection (left). The results displayed on the right account for a modified experimental sequence where laser addressing transfers the atoms to the  $F = 3$  state in a sub-register exclusive fashion, resulting in vanishing fluorescence at the addressed sites. The addressing beam at  $795 \text{ nm}$  is resonant to the transition  $|5S_{1/2}, F = 2\rangle \leftrightarrow |5P_{1/2}, F = 3\rangle$  and is brought to spatial overlap with one of the trapping laser beams by the use of an optical fibre. For the centre trap, we obtain  $p_1 = 0.47(2)$  before and  $p_1 = 0.01(1)$  after the

addressing of the stored atoms. The observed crosstalk is on the order of 2 %, which we contribute to chromatic aberrations.

Individual sites are also addressable by the use of a position-controlled auxiliary laser beam, as displayed in Figure 3(b, bottom). Here, the application of laser light which is resonant to the transition  $|5S_{1/2}, F = 3\rangle \leftrightarrow |5P_{1/2}, F = 3\rangle$  and focused to a spot size of 2  $\mu\text{m}$  leads to a removal of atoms. Repumping light is applied globally during addressing. The initial  $p_1$  of 0.56(2) is converted to  $p_1 = 0.02(1)$  while we do not observe any crosstalk to neighbouring traps. This technique also adds flexibility with respect to the applied wavelength and beam parameters given that a separate beam path is used.

## CONCLUSION

The use of microlens arrays allows for the creation of massive multi-site trap arrays with structure sizes approaching the wavelength of the light applied [21], yet the geometry is decoupled from the trapping laser wavelength and therefore customizable. The presented technique allows for the generation of scalable 2D and 3D arrays with tunable dimensions in the single micrometer regime and thus constitutes a versatile tool for cold atom experiments. Multi-site focused beam arrays enter a regime which has formerly been accessible only by phase-sensitive standing wave configurations, yet they retain the simplicity and robustness of the optical setup as well as their inherent features of single site addressability [54] and coherent quantum state transport [39, 43]. The achieved miniaturization facilitates bottom-up engineering of quantum systems in microlens generated trap arrays and the implementation of coherent multi-atom interactions with direct implications for neutral atom quantum information processing and quantum simulation architectures [10, 12–14, 55].

The implemented Talbot registers provide 161 single-addressable atoms at present with separations well within the limits for Rydberg-mediated interactions. In addition, atomic separations can be precisely adapted using interleaved configurations while sub-register exclusive addressability extends techniques for the initialization and read out of quantum states and allows for the parallelization of operations.

We acknowledge financial support from the Deutsche Forschungsgemeinschaft (DFG) through Grant No. BI 647/6-1 within the Priority Program SPP 1929 (GiRyd).

---

\* gerhard.birkl@physik.tu-darmstadt.de; www.iap.tu-darmstadt.de/apq

- [1] S. Haroche, *Rev. Mod. Phys.* **85**, 1083 (2013).
- [2] D. J. Wineland, *Rev. Mod. Phys.* **85**, 1103 (2013).
- [3] H. Ott, *Reports on Progress in Physics* **79**, 054401 (2016).
- [4] G. Qummer and P. S. Julienne, *Chemical Reviews* **112**, 4949 (2012).
- [5] L. R. Liu, J. D. Hood, Y. Yu, J. T. Zhang, N. R. Hutzler, T. Rosenband, and K.-K. Ni, *Science* **360**, 900 (2018).
- [6] A. D. Ludlow, M. M. Boyd, J. Ye, E. Peik, and P. O. Schmidt, *Rev. Mod. Phys.* **87**, 637 (2015).
- [7] A. D. Cronin, J. Schmiedmayer, and D. E. Pritchard, *Rev. Mod. Phys.* **81**, 1051 (2009).
- [8] D. Budker and M. Romalis, *Nature Physics* **3**, 227 (2007).
- [9] C. L. Degen, F. Reinhard, and P. Cappellaro, *Rev. Mod. Phys.* **89**, 035002 (2017).
- [10] M. Saffman, T. G. Walker, and K. Mølmer, *Rev. Mod. Phys.* **82**, 2313 (2010).
- [11] Folman, R. (ed), *Quantum Information Processing*, Vol. 10 (Springer, 2011) special Issue on Neutral Particles.
- [12] M. Saffman, *Journal of Physics B: Atomic, Molecular and Optical Physics* **49**, 202001 (2016).
- [13] H. Weimer, M. Müller, I. Lesanovsky, P. Zoller, and H. P. Büchler, *Nat Phys* **6**, 382 (2010).
- [14] I. M. Georgescu, S. Ashhab, and F. Nori, *Rev. Mod. Phys.* **86**, 153 (2014).
- [15] S. Kuhr, *National Science Review* **3**, 170 (2016).
- [16] C. Gross and I. Bloch, *Science* **357**, 995 (2017).
- [17] P. Schauss, *Quantum Science and Technology* **3**, 023001 (2018).
- [18] J. Argüello-Luengo, A. González-Tudela, T. Shi, P. Zoller, and J. I. Cirac, arXiv preprint arXiv:1807.09228 (2018).
- [19] I. Bloch, J. Dalibard, and S. Nascimbene, *Nat Phys* **8**, 267 (2012).
- [20] A. Kumar, T.-Y. Wu, F. Giraldo, and D. S. Weiss, *Nature* **561**, 83 (2018).
- [21] M. Schlosser, S. Tichelmann, J. Kruse, and G. Birkl, *Quantum Information Processing* **10**, 907 (2011).
- [22] M. J. Piotrowicz, M. Lichtman, K. Maller, G. Li, S. Zhang, L. Isenhower, and M. Saffman, *Phys. Rev. A* **88**, 013420 (2013).

- [23] B. J. Lester, N. Luick, A. M. Kaufman, C. M. Reynolds, and C. A. Regal, *Phys. Rev. Lett.* **115**, 073003 (2015).
- [24] H. Bernien, S. Schwartz, A. Keesling, H. Levine, A. Omran, H. Pichler, S. Choi, A. S. Zibrov, M. Endres, M. Greiner, *et al.*, *Nature* **551**, 579 (2017).
- [25] H. Kim, Y. Park, K. Kim, H.-S. Sim, and J. Ahn, *Phys. Rev. Lett.* **120**, 180502 (2018).
- [26] D. Barredo, V. Lienhard, S. De Léséleuc, T. Lahaye, and A. Browaeys, *Nature* **561**, 79 (2018).
- [27] C. Sheng, X. He, P. Xu, R. Guo, K. Wang, Z. Xiong, M. Liu, J. Wang, and M. Zhan, *Phys. Rev. Lett.* **121**, 240501 (2018).
- [28] M. A. Norcia, A. W. Young, and A. M. Kaufman, *Phys. Rev. X* **8**, 041054 (2018).
- [29] A. Cooper, J. P. Covey, I. S. Madjarov, S. G. Porsev, M. S. Safronova, and M. Endres, *Phys. Rev. X* **8**, 041055 (2018).
- [30] G. E. Marti, R. B. Hutson, A. Goban, S. L. Campbell, N. Poli, and J. Ye, *Phys. Rev. Lett.* **120**, 103201 (2018).
- [31] S. J. M. Kuppens, K. L. Corwin, K. W. Miller, T. E. Chupp, and C. E. Wieman, *Phys. Rev. A* **62**, 013406 (2000).
- [32] R. Dumke, M. Volk, T. Mütter, F. B. J. Buchkremer, G. Birkl, and W. Ertmer, *Phys. Rev. Lett.* **89**, 097903 (2002).
- [33] F. Serwane, G. Zürn, T. Lompe, T. B. Ottenstein, A. N. Wenz, and S. Jochim, *Science* **332**, 336 (2011).
- [34] M. McGovern, A. J. Hilliard, T. Grünzweig, and M. F. Andersen, *Opt. Lett.* **36**, 1041 (2011).
- [35] N. Schlosser, G. Reymond, I. Protsenko, and P. Grangier, *Nature* **411**, 1024 (2001).
- [36] T. Grünzweig, A. Hilliard, M. McGovern, and M. F. Andersen, *Nat. Phys.* **6**, 951 (2011).
- [37] M. Schlosser, J. Kruse, and G. Birkl, arXiv preprint arXiv:1902.00370 (2019).
- [38] J. Beugnon, C. Tuchendler, H. Marion, A. Gaëtan, Y. Miroshnychenko, Y. R. Sortais, A. M. Lance, M. P. Jones, G. Messin, A. Browaeys, *et al.*, *Nature Physics* **3**, 696 (2007).
- [39] A. Lengwenus, J. Kruse, M. Schlosser, S. Tichelmann, and G. Birkl, *Phys. Rev. Lett.* **105**, 170502 (2010).
- [40] D. Barredo, S. de Léséleuc, V. Lienhard, T. Lahaye, and A. Browaeys, *Science* **354**, 1021 (2016).
- [41] M. Endres, H. Bernien, A. Keesling, H. Levine, E. R. Anschuetz, A. Krajenbrink, C. Senko, V. Vuletic, M. Greiner, and M. D. Lukin, *Science* **354**, 1024 (2016).

- [42] W. Lee, H. Kim, and J. Ahn, *Phys. Rev. A* **95**, 053424 (2017).
- [43] D. O. de Mello, D. Schäffner, J. Werkmann, T. Preuschoff, L. Kohfahl, M. Schlosser, and G. Birkl, arXiv preprint arXiv:1902.00284 (2019).
- [44] A. M. Kaufman, B. J. Lester, C. M. Reynolds, M. L. Wall, M. Foss-Feig, K. R. A. Hazzard, A. M. Rey, and C. A. Regal, *Science* **345**, 306 (2014).
- [45] S. Murmann, A. Bergschneider, V. M. Klinkhamer, G. Zürn, T. Lompe, and S. Jochim, *Phys. Rev. Lett.* **114**, 080402 (2015).
- [46] M. R. Sturm, M. Schlosser, R. Walser, and G. Birkl, *Phys. Rev. A* **95**, 063625 (2017).
- [47] M. R. Sturm, M. Schlosser, G. Birkl, and R. Walser, *Phys. Rev. A* **97**, 063608 (2018).
- [48] A. Browaeys, D. Barredo, and T. Lahaye, *Journal of Physics B: Atomic, Molecular and Optical Physics* **49**, 152001 (2016).
- [49] J. Wen, Y. Zhang, and M. Xiao, *Adv. Opt. Photon.* **5**, 83 (2013).
- [50] C. Mennerat-Robilliard, D. Boiron, J. M. Fournier, A. Aradian, P. Horak, and G. Grynberg, *EPL (Europhysics Letters)* **44**, 442 (1998).
- [51] Y. B. Ovchinnikov, *Phys. Rev. A* **73**, 033404 (2006).
- [52] B. Besold and N. Lindlein, *Optical Engineering* **36**, 1099 (1997).
- [53] H. Kim, W. Lee, H. Lee, and J. Ahn, *Phys. Rev. A* **91**, 033817 (2015).
- [54] J. Kruse, C. Gierl, M. Schlosser, and G. Birkl, *Phys. Rev. A* **81**, 060308 (2010).
- [55] A. W. Glaetzle, R. M. van Bijnen, P. Zoller, and W. Lechner, *Nature Communications* **8**, 15813 (2017).